Building Blocks of Eumelanin: Relative Stability and Excitation Energies of Tautomers of 5,6-Dihydroxyindole and 5,6-Indolequinone

Yuri V. Il'ichev*,† and John D. Simon‡

Department of Chemistry, Wichita State University, 1845 Fairmount, Wichita, Kansas 67260-0051 and Departments of Chemistry and Biochemistry, Duke University, Durham, North Carolina 27708

Received: March 18, 2003; In Final Form: May 27, 2003

Computation methods were used to examine the tautomerization equilibria for 5,6-dihydroxyindole (DHI, **2**) and 5,6-indolequinone (IQ, **3**). Relative energies were calculated at the B3LYP and PBE0 level of theory; solvent effects were modeled by using the CPCM method. Nine tautomers of **2** were examined. Our data showed that the generally accepted molecular structure of **2** corresponds to the most stable tautomer in both gas phase and aqueous solution. In aqueous solution, the quinone methide tautomer was the second most stable structure, being destabilized by 6 kcal mol^{-1}. In contrast, gas-phase DFT calculations on four tautomers of **3** suggest this compound exists as a mixture of two tautomers, the quinone and the quinone methide. The relative concentration of the quinone methide is predicted to be sufficient to be detected experimentally. The energy difference between these two tautomers increases in solution so concentration of quinone methide should be negligible in polar solvents. Vertical excitation energies for tautomers of **2** and **3** in solutions were obtained by combining TD-DFT techniques with the SCRF−CPCM calculations. Simulated absorption spectra in water were in semiquantitative agreement with available experimental data. Relatively strong absorption in near-IR range was predicted for **3**. This spectral feature might be used to clarify the complex mechanisms of dihydroxyindole oxidation.

Introduction

Melanin refers to a group of biological pigments.[1] The most ubiquitous melanin in mammals is the black eumelanin, which is largely comprised of substituted indolic units derived from the oxidation of tyrosine. Given that melanins are some of the most abundant natural pigments, it may appear surprising their chemical structures and biological roles are still subject to debate. However, to date, it has proven impossible to assign a unique molecular structure to melanin. Scheme 1 shows the current understanding of initial steps of the molecular mechanism for the formation of eumelanins.[1−3] The first step of melanogenesis is the enzymatic hydroxylation of tyrosine. Through a series of oxidative reactions, the key intermediate dopachrome (**1b** in Scheme 1) is generated. Tautomerization of **1b** affords the enol form of 5,6-dihydroxy-2-indolecarboxylic acid (DHICA, **1a**). The isomerization reaction may also be accompanied by decarboxylation and lead to 5,6-dihydroxyindole (DHI, **2a**). Oxidation of **1a** and **2a** results in the formation of the corresponding indolequinones, IQCA and IQ (**3a**). These molecules together with **1a** and **2a** are often cited as the molecular precursors of eumelanin because they are believed to be involved in the polymerization reaction affording the pigment.

In this paper, we examine the molecular structure of DHI, **2**, and IQ, **3**. These two molecules are presented in Scheme 1 and Figure 1 as single tautomers. There are multiple possibilities for keto−enol and imine−enamine tautomerization of these compounds. Tautomerization equilibria may play an important role in the chemistry and spectroscopy of dihydroxyindoles and the corresponding quinones and the resulting melanin structure. To our best knowledge, there is no direct experimental evidence for the presence of minor tautomers of **2** in measurable quantities (>0.001%) under equilibrium conditions. However, this does not exclude their formation as transients or their presence at much higher concentration when **2** is incorporated into melanin pigments. Fundamental importance of tautomerization of dihydroxyindoles for melanin synthesis in vivo is generally recognized (see Scheme 1).[1,2]

Pulse radiolysis was utilized by two different groups[4,5] to establish mechanism of oxidation of **2** and its analogues. On the basis of only transient absorption data, both groups claimed to obtain evidence for the formation of **3** and even its tautomerization into more favorable quinone methide or quinone imine. From subsequent studies of monohydroxyindoles and partly methylated analogues of **2**, which were unable to form 5,6-quinone, Al-Kazwini et al.[6] concluded a relatively stable intermediate with an absorption maximum around 430 nm was quinone methide. Basically, the same conclusion was made by Lambert et al.[7] upon a comparative study of the oxidation of 6-hydroxy-5-methoxyindole and 5-hydroxy-6-methoxyindole. However, these workers suggested that transient absorption above 400 nm observed in irradiated solutions of 6-hydroxy-5-methoxyindole was largely due to the protonated form of the quinone methide. Although tentative spectral assignment made by these two groups[4−7] apparently was corroborated by their results obtained with analogues of **2**, it has not yet been confirmed by independent experimental studies or computational data. Unambiguous identification of intermediates and unraveling mechanisms of dihydroxyindole oxidation requires additional experimental and computational work.

Computational studies of model polymers and small molecules related to eumelanin were pioneered by Pullman and

* To whom correspondence should be addressed. Tel: 316-978-5702; fax: 316-978-3431; e-mail: Yuri.Ilitchev@wichita.edu.
† Wichita State University.
‡ Duke University.

10.1021/jp034702x CCC: $25.00
Published on Web 07/08/2003

SCHEME 1: Molecular Mechanism for Early Steps of the Formation of Eumelanins[a]

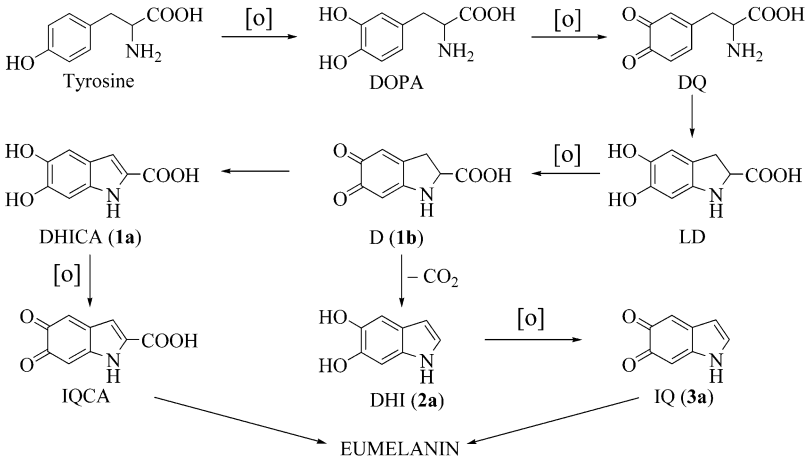

[a] DOPA, 3,4-dihydroxyphenylalanine; DQ, dopaquinone; LD, leucodopachrome; D, dopachrome; DHICA, 5,6-dihydroxyindole-2-carboxylic acid; IQCA, 5,6-indolequinone-2-carboxylic acid; DHI, 5,6-dihydroxyindole; IQ, 5,6-indolequinone.

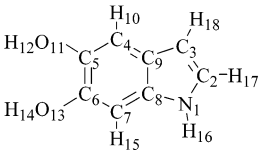

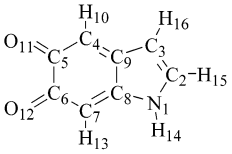

Figure 1. Molecular structures of DHI (**2a)** and IQ (**3a)**. Atom numbering used in this work is shown.

Pullman.[8] By using semiempirical techniques, Caldas and coworkers[9,10] later obtained interesting results that suggested certain properties of eumelanin pigments could be understood from computed properties of model oligomers. The same group also applied ab initio techniques to obtain optimized geometries of a single tautomer of **2** and two tautomers of **3** in different charge states. The DFT techniques were recently utilized by Stark et al.[11] to obtain geometries of the same three molecules. The later results were found to be in good agreement with the HF results of Bolívar-Marinez et al.[10] Two different semiempirical techniques applied by these two groups to predict optical absorption spectra of the selected monomers provided generally consistent results. However, when a measured spectrum of **2** was compared to that calculated for a particular tautomer, such as shown in Scheme 1 and Figure 1, significant discrepancies were found.[11] Because relative stability of different tautomers was not assessed, it remained unclear whether these discrepancies were just due to computational deficiencies or due to the presence of several tautomers in a solution of **2**. Surprisingly, both Bolívar-Marinez et al.[10] and Stark et al.[11] referred to the second selected tautomer of **3** (quinone imine) with zero charge as the reduced form of 5,6-indolequinone. One-electron reduction of **3** with subsequent protonation of the semiquinone radical anion should afford a radical that might be represented by a similar structure, but it must have an additional hydrogen atom.

The major goal of this computational study is evaluation of relative stabilities of tautomers of **2** and **3** in different environments. In addition, we used time-dependent DFT to predict absorption spectra of these compounds in different tautomeric forms as an initial step toward understanding optical spectra of melanin pigments and its precursors in vivo. Identification of the most stable tautomers is of primary importance not only for successful application of computational techniques to prediction of properties of dihydroxyindole polymers but also for interpretation of experimental data for such complex systems as melanin pigments. Our computational results related to the tautomerization and protolytic equlibria of **1** will be reported elsewhere.

Computational Methods

All calculations were performed with Gaussian 98 package of programs.[12] Tautomer geometries were initially optimized with the AM1 method. Final geometries were obtained upon full optimization at the B3LYP level of theory with the 6-31G-(d) basis set. Single-point energies for these geometries were computed by using the B3LYP and PBE0 hybrid functionals with the 6-311+G(2d,p) and 6-311++G(d,p) basis sets. B3LYP is a combination of Becke's three-parameter exchange functional[13] with the slightly modified Lee−Yang−Parr[14] (LYP) correlation functional. PBE0 (also referred to as PBE1PBE) is a hybrid functional recently implemented in Gaussian 98. This model is obtained by combining a predetermined amount of exact exchange with the Perdew−Burke−Ernzerhof exchange and correlation functionals.[15,16] For all stationary points, the wave function stability was tested and harmonic vibrational frequencies were calculated using analytical second derivatives.

Electronic absorption spectra of different tautomers were estimated on the basis of excitation energy calculations using the random-phase approximation for a time-dependent DFT calculation.[17] The B3LYP and PBE0 methods were used for TD-DFT computations performed in the gas phase and in solution. Self-consistent reaction field (SCRF) calculations were employed to estimate solvent effects on the energies. The polarizable conductor calculation model (CPCM)[18] was employed in these calculations. Acetonitrile ($\epsilon = 36.6$) and water ($\epsilon = 78.4$) were selected as solvents. The scaling factor for solvent accessible surfaces and the initial number of tesserae on the surface of each sphere were set to default values of 1.2 and 60, respectively.

Results and Discussion

Structure and Stability of Tautomers of 5,6-Dihydroxyindole (2). Initial estimates for geometries and energies of

tautomers of **2** were obtained with the AM1 method. Fifteen structures differing in the position of two hydrogen atoms were optimized. Only conformers stabilized by an intramolecular hydrogen bond were considered. Nine tautomers with the lowest enthalpy of formation were selected for geometry optimization at the B3LYP/6-31G(d) level of theory, which is known to provide reliable geometries.[19−22] The molecular structures of these tautomers along with computed dipole moments and relative energies are presented in Figure 2. All of the remaining tautomers could be obtained by displacing a hydrogen atom from an oxygen atom to the nitrogen in one of the nine selected isomers. Zwitterionic character of these structures suggests strong stabilization in aqueous solution. However, our results for **2f** and **2i**, which had comparable dipole moments (see below), indicated that these zwitterions should be still destabilized by more than 15 kcal mol^{-1} in comparison to **2a**. To obtain more accurate estimates of relative stabilities of **2a**−**2i**, we used larger basis sets to compute single-point energies at the B3LYP/6-31G(d) geometries. In addition to the B3LYP method, we also used a novel hybrid model PBE0 in combination with the 6-311++G(d,p) basis set. The relative energies were calculated from absolute energies corrected to the zero-point vibrational energies scaled by 0.9806.[23] The results are collected in Table 1. For tautomers **2a**−**2c**, geometries and energies of two conformers differing in the in-plane orientation of the two hydroxyl groups were obtained. Figure 2 shows the conformer of **2a** that was stabilized by ∼0.8 kcal mol^{-1} relative to that with the OH groups rotated by 180°. On the basis of these results, we also selected for presentation analogous conformers of **2b** and **2c** although they were slightly less favorable (0.4−0.7 kcal mol^{-1}) than those with the OH groups rotated.

Free energies in solution were determined for six tautomers, **2a**, **2b**, **2d**, **2e**, **2f**, and **2i**, which had the lowest B3LYP/6-311+G(2d,p) energies in the gas phase. Although no clear-cut distinction between **2c** and the selected molecules **2f** and **2i** could be made on the basis of their energies, we excluded **2c** from the further study because it was predicted to have a smaller dipole moment and therefore no pronounced solvation effects were anticipated. Properties of **2f** are of immediate interest for melanin studies because its analogue **1b** is believed to be the major precursor of 5,6-dihydroxyindole in melanogenesis in vivo.[1] Bulk solvent effects were initially estimated by using the single-point energies computed for the gas-phase geometries in the framework of the SCRF−CPCM model. Finally, geometries of three isomers (**2a**, **2e**, and **2f**) were optimized at the B3LYP/6-31G(d) level using the CPCM model and water as a solvent. Again, these geometries were utilized to calculate single-point energies in water at the B3LYP and PBE0 level of theory with the 6-311++G(d,p) basis set. The results are summarized in Table 1. The Cartesian coordinates and total energies for all stationary points are available as Supporting Information. Both methods in water yielded identical energies for the two conformers of **2a** differing in the orientation of the two hydroxyl groups.

The B3LYP geometry optimization yielded an essentially planar structure for the indole moiety of all the tautomers of **2** except **2f**. The five-membered ring in **2f** adopted an envelope-like conformation with the C_2 atom displaced from the plane of the benzene ring. Prediction of the completely planar structure of **2a** is in agreement with DFT results of Stark et al.[11] and semiempirical data obtained in this work and in ref 10. The computed bond lengths of **2a** when compared with those determined for tryptophan (Trp) in a crystallographic study[24] showed a significant elongation of **2a** along the short pseudo-

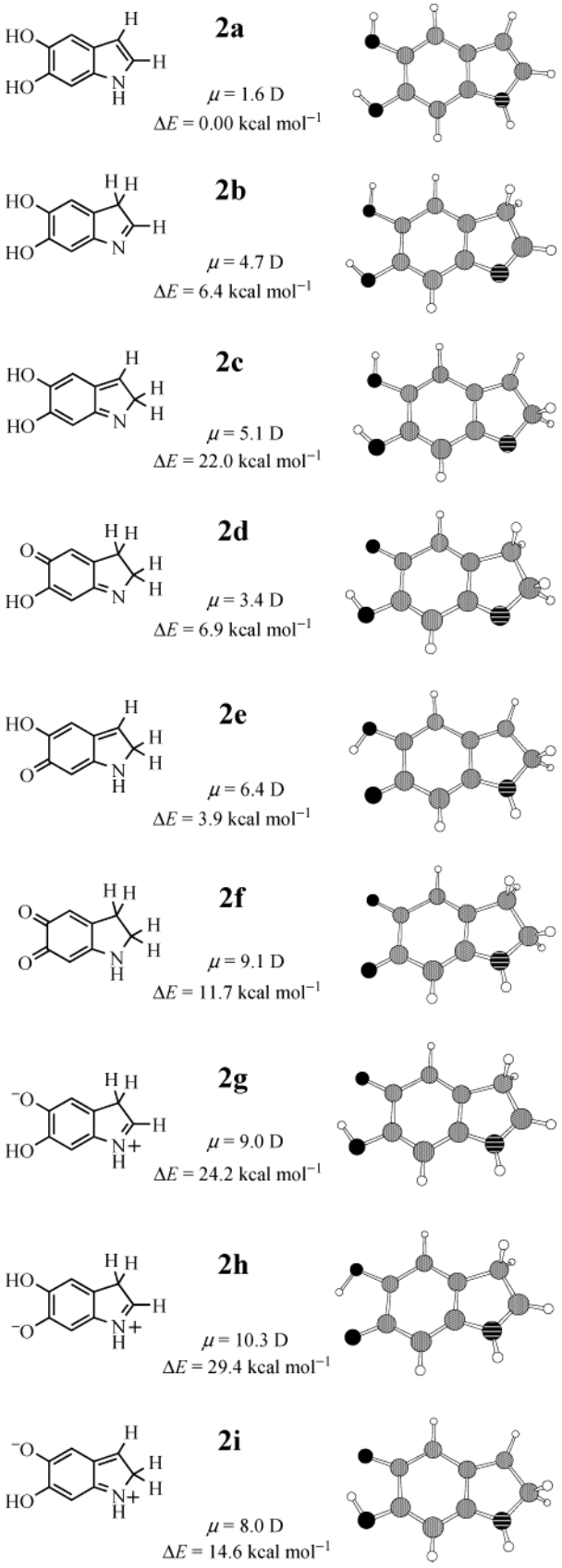

Figure 2. The B3LYP/6-31G(d) optimized geometries, dipole moments, and relative energies in kcal mol^{-1} for selected tautomers of **2**.

symmetry axis of the indole. The B3LYP results gave a bond length of 1.420 Å for both C_5-C_6 and C_8-C_9 bond. The X-ray data for Trp provided values of 1.386 Å and 1.380 Å for these two bonds, respectively. The C_2-C_3 bond in **2a** was also

TABLE 1: Energies of Tautomers of 5,6-Dihydroxyindole (2) in fcal mol^{-1} Relative to That of 2a[a]

method[b]	medium[c]	**2b**	**2c**	**2d**	**2e**	**2f**	**2g**	**2h**	**2i**
A	V	2.7	23.3	14.9	15.7	12.7	28.2	39.8	38.0
B	V	6.4	22.0	6.9	3.9	11.7	24.2	29.4	14.6
C	V	8.6	23.9	13.4	7.8	20.0	27.2	31.9	18.3
D	V	9.4	24.8	14.9	8.7	20.2	27.9	32.8	19.5
D	N	9			7				
D	W	8		18	6	14			14
E	V	10.3		17.5	10.1	23.5			19.5
E	N	10			8				
E	W	9		21	8	18			16
F	W				3	6			
G	W				6	13			

[a] Relative energy was calculated as a difference either between single-point energies corrected to the scaled zero-point energies or between free energies in solution. [b] A, AM1; B, B3LYP/6-31G(d)// B3LYP/6-31G(d); C, B3LYP/6-311+G(2d,p)// B3LYP/6-31G(d); D, B3LYP/6-311++G(d,p)//B3LYP/6-31G(d); E, PBE0/ 6-311++G(d,p)// B3LYP/6-31G(d); F, B3LYP/6-31G(d)//B3LYP/6-31G(d), geometry optimized in water with the SCRF−CPCM method; G, B3LYP/6-311++G(d,p)// B3LYP/6-31G(d), geometry optimized in water with the SCRF−CPCM method. [c] V, vacuum (gas phase); N, acetonitrile; W, water; solvent effects were estimated with the SCRF−CPCM method.

predicted to be stretched by 0.026 Å relative to that in Trp. Similar discrepancies between calculated and experimental C−C bond lengths were also noticed in recent high-level computational studies of indole.[25] Surprisingly, the HF method with the different basis sets yielded values of the C_8-C_9 bond length (∼1.39 Å[10,25a]) which were much closer to the experimental one. The comparable bond lengths obtained in this study from the B3LYP/6-31G(d) optimized geometries of **2a** and indole[26] were practically identical to each other and to those in **2a** obtained at the LDA/VWN and GGA/BP levels of theory.[11]

Dopachrome (**1b**) has often been depicted as a zwitterion with the formally double $N-C_8$ and C_6-C_7 bonds. According to our B3LYP data, the $N-C_8$ bond in **2f** (1.367 Å) was strongly elongated in comparison to that in **2d** (1.296 Å) and only slightly shortened relative to that in **2a** (1.381 Å). A much larger value of 1.464 Å was obtained for the $N-C_2$ bond length in **2f**. The C_6-C_7 bond in this molecule (1.450 Å) was much longer than the C_7-C_8 bond (1.364 Å). These data suggested stronger coupling of the N atom to the six-membered ring in **2f** as compared to **2a** but the resonance structure shown in Figure 2 appeared to be more suitable for the representation of this molecule than the zwitterionic structure.

Our DFT calculations performed with two different functionals and three different basis sets in the gas phase and in solution identified **2a** and **2e** as the most stable tautomers. The relative energies that were calculated from the B3LYP/ 6-311+G(2d,p) data were slightly lower than those obtained with the 6-311++G(d,p) basis set at the same level of theory. Generally, destabilization of minor tautomers was overestimated by 1−3 kcal mol^{-1} when the PBE0 single-point energies were used instead of the B3LYP ones. The energy order predicted at the B3LYP level with a relatively small basis set 6-31G(d) was essentially the same as that found with two larger basis sets. In contrast, semiempirical calculations resulted in a largely different picture of the tautomer stability. Our DFT results confirmed a common view that 5,6-dihydroxyindole exists mainly as enol **2a**. According to our best estimate for the gas phase and aqueous solution, the quinone methide **2e** was destabilized by more than 6 kcal mol^{-1}, respectively. The smallest energy difference between **2a** and **2e** in water allowed us to estimate relative concentration of **2e** at the level of ∼0.005% which is close to the detection limit of the vast majority of analytical techniques. The predicted stability order in the series **2a**, **2e**, **2f** was in good agreement with the proposed mechanism of the spontaneous isomerization of **1b** into the enol form. Formation of relatively stable quinone methides upon tautomerization of substituted aminochromes has been reported by several groups.[27] These compounds have been obtained by oxidation of α-methyl-3,4-dihydroxyphenylalanine esters. Later, Prota and co-workers[28] used kinetic isotope effect to demonstrate that formation of the quinone methide is the primary step in the isomerization of **1b**. Subsequent tautomerization and decarboxylation of this methide affords **2a**. Assuming that substitution does not change dramatically the relative energies of the tautomers, these data imply an increase in the thermodynamic stability in the series 2,3-dihydroindole-5,6-quinone (**2f**), quinone methide (**2e**), dihydroxyindole (**2a**). The computational data (see Table 1) confirmed this conclusion. Tautomerization involving carbon atoms are very slow, even for highly exothermic processes. In protic solvents, reactions involving H-transfer between heteroatoms, such as **2f** → **2d**, may therefore efficiently compete with the tautomerization involving a carbon atom. We found that in the gas phase **2d** was more favorable than **2f** by 5−7 kcal mol^{-1}. However, for aqueous solution both DFT techniques predicted for **2d** to be destabilized by 3−4 kcal mol^{-1} relative to **2f**. We concluded that rearrangement of **2f** in water proceeds via formation of **2e** as suggested for the substituted analogue **1b**. However, in nonpolar environments another mechanism including such intermediates as **2d** and **2b** represents a feasible alternative for the isomerization of 2,3-dihydroindole-5,6-quinones.

Excitation Energies of Tautomers of 5,6-Dihydroxyindole (2). Vertical excitation energies for the 10 lowest excited states of singlet multiplicity were obtained for the four tautomers of **2** by using TD-DFT calculations at the B3LYP or PBE0 level with the 6-311++G(d,p) basis set. The results are presented in Table 2. The excitation energies obtained with the B3LYP method were generally underestimated in comparison to those predicted with the PBE0 model. The later method has recently been shown to provide rather accurate description of low-lying excited states.[16,29]

According to the TD-B3LYP results, the six lowest electronic transitions in **2a** had energies in the range 4.3−4.8 eV (288−249 nm). Transitions to S_1, S_3, S_4, and S_6 were predicted to be extremely weak (oscillator strength $f < 0.003$) and to have dipole moments almost perpendicular to the molecular plane. The two most intense features of the electronic spectrum were found at 4.43 (280 nm) and 4.65 eV (267 nm) as in-plane transitions, S_2 and S_5, whose transition dipole moments were almost parallel to the long and short pseudoaxis of the substituted indole, respectively. The TD-DFT computations at the B3LYP level in combination with the CPCM model predicted energies of 4.45 eV (278 nm) and 4.60 eV (270 nm) for the two lowest excited states of **2a** in water, the strength and orientation of the dipole moment for these transitions were similar to those for S_2 and S_5 in the gas phase. No significant change in the vertical excitation energies was obtained when the geometry of **2a** optimized in water was used instead of the gas-phase optimized geometry. Energies of 4.44 and 4.58 eV were obtained for S_1 and S_2 transitions at the B3LYP/6-311++G(d,p) level. TD-DFT results obtained for another conformer of **2a** with the two OH groups rotated by 180° were generally very similar in terms of absolute energies. However, the reversed order of S_2 and S_3 states and slightly different orientation of the transition moments for the two most intense features were predicted for the later

TABLE 2: Vertical Excitation Energies in eV and Oscillator Strengths (Numbers in Brackets) for Singlet Excited States of Different Tautomers of 5,6-Dihydroxyindole (2)

	a	*b*	S_1	S_2	S_3	S_4	S_5	S_6	S_7	S_8	S_9	S_{10}
2a	V	D	4.30	4.43	4.47	4.60	4.65	4.84	4.99	5.25	5.34	5.38
			(0.0003)	(0.160)	(0.003)	($<10^{-4}$)	(0.036)	(0.0001)	(0.002)	(0.002)	(0.0002)	(0.0009)
	V	E	4.53	4.60	4.74	4.77	4.89	5.12	5.24	5.50	5.60	5.66
			(0.168)	(0.0002)	(0.003)	(0.041)	(0.000 1)	(0.0001)	(0.003)	(0.002)	(0.0004)	(0.001)
	W	D	4.45	4.60	4.65	4.87	4.96	5.20	5.22	5.46	5.57	5.71
			(0.149)	(0.037)	(0.0004)	(0.005)	(0.005)	(0.0004)	(0.0001)	($<10^{-4}$)	(0.0009)	(0.003)
	W	E	4.56	4.72	4.91	5.14	5.25	5.48	5.51	5.75	5.85	5.88
			(0.156)	(0.042)	(0.0008)	(0.005)	(0.004)	(0.0005)	($<10^{-4}$)	($<10^{-4}$)	(0.001)	(0.177)
2b	V	D	4.23	4.44	4.50	4.98	5.06	5.28	5.32	5.39	5.72	5.78
			(0.084)	(0.0001)	(0.003)	(0.001)	(0.003)	(0.370)	(0.0004)	(0.0009)	(0.068)	(0.082)
	V	E	4.38	4.62	4.72	5.07	5.33	5.45	5.60	5.68	5.86	6.05
			(0.095)	(0.004)	(0.0001)	(0.001)	(0.002)	(0.389)	($<10^{-4}$)	(0.002)	(0.080)	(0.0008)
	W	D	4.24	4.55	4.88	5.23	5.27	5.33	5.57	5.80	5.80	5.93
			(0.102)	(0.002)	($<10^{-4}$)	(0.001)	(0.310)	(0.004)	($<10^{-4}$)	(0.039)	(0.045)	(0.0005)
	W	E	4.40	4.67	5.15	5.31	5.46	5.61	5.85	5.94	6.09	6.21
			(0.115)	(0.003)	($<10^{-4}$)	(0.001)	(0.325)	(0.003)	($<10^{-4}$)	(0.101)	($<10^{-4}$)	(0.0006)
2e	V	D	3.17	3.73	4.04	4.81	5.01	5.37	5.50	5.55	5.67	5.71
			(0.006)	($<10^{-4}$)	(0.408)	(0.0003)	(0.001)	(0.002)	(0.027)	($<10^{-4}$)	(0.0001)	(0.034)
	V	E	3.27	3.83	4.14	5.09	5.29	5.66	5.69	5.82	5.90	5.91
			(0.007)	($<10^{-4}$)	(0.442)	(0.0005)	(0.001)	(0.002)	(0.022)	(0.0001)	(0.042)	(0.047)
	W	D	3.27	4.10	4.15	5.22	5.44	5.46	5.59	5.68	5.72	5.74
			(0.018)	(0.385)	(0.0001)	(0.001)	(0.002)	(0.038)	($<10^{-4}$)	(0.072)	(0.004)	(0.0002)
	W	E	3.37	4.20	4.24	5.47	5.65	5.68	5.84	5.86	5.89	6.02
			(0.019)	(0.417)	(0.0001)	(0.001)	(0.032)	(0.002)	(0.079)	(0.016)	(0.0002)	(0.0002)
2f	V	D	2.04	2.75	3.27	4.43	4.90	4.92	5.20	5.39	5.46	5.50
			($<10^{-4}$)	(0.046)	($<10^{-4}$)	(0.183)	(0.002)	(0.0003)	(0.0001)	(0.069)	(0.036)	(0.003)
	V	E	2.09	2.85	3.38	4.55	5.09	5.16	5.56	5.61	5.69	5.73
			($<10^{-4}$)	(0.049)	($<10^{-4}$)	(0.202)	(0.0004)	(0.002)	(0.014)	(0.086)	(0.0005)	(0.021)
	W	D	2.40	2.53	3.70	4.07	5.41	5.44	5.51	5.81	5.95	5.98
			(0.0005)	(0.042)	(0.0001)	(0.229)	(0.062)	(0.015)	(0.006)	(0.008)	($<10^{-4}$)	(0.101)
	W	E	2.44	2.63	3.80	4.18	5.57	5.60	5.74	5.93	6.11	6.14
			(0.0003)	(0.046)	(0.0001)	(0.246)	(0.029)	(0.057)	(0.006)	(0.004)	(0.003)	(0.195)

[a] Medium: V, vacuum (gas phase); W, water; solvent effects were estimated with the SCRF−CPCM method. [b] Level of theory: see footnote for Table 1.

conformer in the gas phase. Very similar spectra of the two conformers were found in acetonitrile and water. The PBE0 calculations yielded the reversed energy order for S_1/S_2 and S_4/S_5 transitions of **2a** in the gas phase. The vertical excitation energies of 4.56 eV (272 nm) and 4.72 eV (263 nm) were obtained at the PBE0/6-311++G(d,p) level for the two lowest excited states of **2a** in water. Notice that results of the PBE0 model for the transition moment orientations and oscillator strengths corresponding to S_1 and S_2 of **2a** in water and acetonitrile (data not shown) were essentially the same as those obtained with the B3LYP functional.

The electronic absorption spectrum of **2** in water contains two major features with maxima around 274 nm ($\epsilon = 5150$ $M^{-1}m^{-1}$) and 299 nm ($\epsilon = 7290$ $M^{-1}m^{-1}$).[30] The spectrum of **2a** simulated by using the TD-DFT results (see Table 2 and Figure 3) was in qualitative agreement with the measured one which contained two strongly overlapping bands with the stronger transition having the lower energy. However, the absolute energy of the S_1 state seemed to be considerably overestimated with both computational methods used. An additional strong feature that was found around 220 nm only for the most stable conformer of **2a** with the PBE0 method (Figure 3) is in good agreement with experimental data.[30] It is well known that the indole chromophore represents a real challenge both for experimental and computational studies (see ref 25 and references therein). Spectroscopic properties of the parent compound had attracted considerable interest and often received contradictory accounts.[25,31] Accurate experimental determination and theoretical prediction of the origins of the two close-lying S_1 and S_2 states of indole has proven to be difficult.

It is of interest to compare the predicted absorption spectra of **2a** and **2e**, the most favorable minor tautomer. As can be seen from Figure 3, the spectrum of **2e** is expected to be strongly shifted to the red in comparison to that of **2a**. The PBE0 method predicted a rather weak $S_0 \rightarrow S_1$ transition at 379 nm (3.27 eV) and 368 nm (3.37 eV) for **2e** in a vacuum and in water, respectively. The B3LYP calculations yielded vertical excitation energies of 3.17 eV (391 nm) and 3.27 eV (379 nm). Both the PBE0 and B3LYP method predicted the strongest band in the spectrum to be around 300 nm. In addition, relatively strong absorption was found around 210−220 nm. The two later transitions were predicted to be largely insensitive to environment. The simulated spectrum of the quinone methide **2e** might be compared to that of a relatively stable methide obtained from a substituted aminochrome. The electronic absorption spectrum of the quinone methide derived from α-methyldopamethyl ester had maxima at 221, 313, and 420 nm[27c] and showed striking resemblance to the spectrum of **2e** simulated by using the B3LYP data. Although the computed energy of the $S_0 \rightarrow S_1$ transition was significantly overestimated relative to that of the measured absorption maximum, **2e** was the only tautomer that showed appreciable absorbance in the range 370−420 nm (see Figure 3).

As mentioned above, **2f** is the decarboxylated analogue of dopachrome **1b**. The later compound was identified as a major intermediate of melanogenesis which had an electronic absorp-

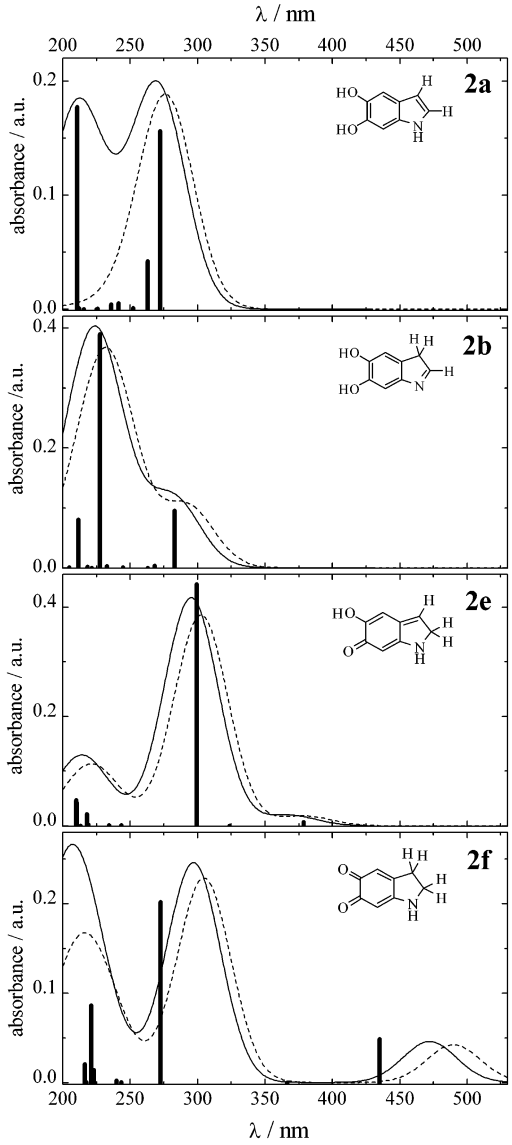

Figure 3. Calculated absorption spectra of **2a**, **2b**, **2e**, and **2f** in the gas phase (vertical bars) and in aqueous solution (solid and dashed lines). The spectra in solution were simulated by using Gaussian envelopes centered at the computed absorption maxima with arbitrary width of 20 nm and amplitude equal to the oscillator strength. The PBE0 (solid) and B3LYP method (dashed) were used in combination with the 6-311+G(d,p) basis set and the CPCM model.

tion spectrum peaked at 475 nm. Formation of a relatively stable intermediate (~10 s) with absorption maximum around 470 nm was reported by Al-Kazwini et al.[32] in a pulse radiolysis study of 5,6-dihydroxy-2,3-dihydroindole oxidation. This intermediate was assigned to a decarboxylated analogue of **1a**, that is, **2f**. Our results obtained with the B3LYP and PBE0 methods suggested that $S_0 \rightarrow S_1$ transition in **2f** should be very weak and show a significant solvatochromic shift to the blue. In contrast, the transition to the S_2 state was predicted to be relatively strong and to show a batochromic shift with solvent polarity (see Table 2 and Figure 3). The transition dipole moment was in the plane of the benzene ring and directed approximately parallel to C_7-C_8 bond. The vertical transition energy corresponding to $S_0 \rightarrow S_2$ for **2f** in water was predicted to be 2.53 eV (490 nm) and 2.63 eV (472 nm) at the B3LYP and PBE0 level, respectively. The two most intense features of the **2f** spectrum were around 300 and 210 nm. The PBE0 result for the lowest energy transition is in excellent agreement with the measured absorption maxima for the intermediate of 5,6-dihydroxy-2,3-dihydroindole oxidation and for **1b**. Our preliminary results obtained at the same levels of theory provided essentially the same absorption maxima for a selected conformer of **1b** (469 nm)[26] and for **2f** (472 nm).

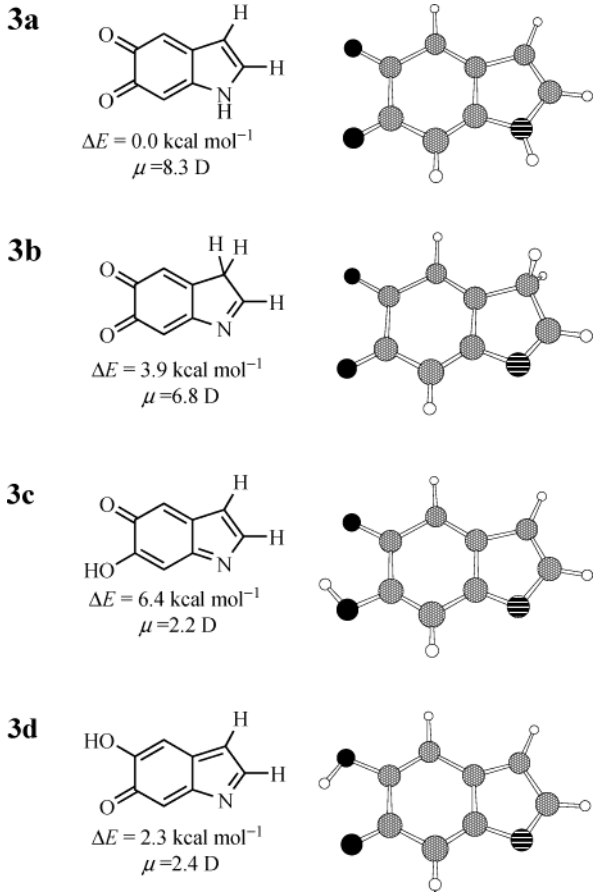

Figure 4. The B3LYP/6-31G(d) optimized geometries, dipole moments, and relative energies in kcal mol^{-1} for tautomers of **3**.

TABLE 3: Energies of Tautomers of 5,6-Indolequinone (3) in kcal mol^{-1} Relative to That of 3a[a]

method[b]	medium[c]	3b	3c	3d
A	V	−1.5	9.0	6.4
B	V	3.9	6.4	2.3
C	V	6.1	4.3	0.6
D	V	6.9	5.7	1.9
D	N	8	12	7
D	W	8	12	8
E	V	7.5	5.4	1.4
E	N	9	11	7
E	W	9	12	7
F	W	6		8
G	W	8		8

[a,b,c] See footnotes for Table 1.

Structure and Stability of Tautomers of 5,6-Indolequinone (3). Four tautomers of **3** were initially optimized at the AM1 level. Surprisingly, the most stable compound was predicted to be **3b** (see Figure 4 and Table 3). Subsequently, all geometries were fully optimized at the B3LYP/6-31G(d) level of theory. The molecular structures of the tautomers of **3** along with dipole moments and relative energies computed at this level are presented in Figure 4 and Table 3. The DFT results suggested **3a** was the most stable compound in the series studied. This conclusion was confirmed by the single-point energy calculations both at the B3LYP and PBE0 level with larger basis sets (see Table 3). However, the DFT methods predicted the energy of quinone methide **3d** in the gas phase to be very close to that

TABLE 4: Vertical Excitation Energies in eV and Oscillator Strengths (Numbers in Brackets) for Singlet Excited States of Different Tautomers of 5,6-Indolequinone (3)

	a	*b*	S_1	S_2	S_3	S_4	S_5	S_6	S_7	S_8
3a	V	D	1.79	1.99	3.03	4.16	4.65	4.66	4.85	5.07
			(<10^{-4})	(0.033)	0.0000	(0.048)	(0.065)	(0.0008)	(<10^{-4})	(0.152)
	V	E	1.82	2.06	3.13	4.30	4.79	4.92	5.01	5.24
			(<10^{-4})	(0.036)	(<10^{-4})	(0.050)	(0.076)	(0.0009)	(<10^{-4})	(0.167)
	W	D	1.57	2.08	3.39	3.80	4.40	4.91	5.20	5.31
			(0.019)	(<10^{-4})	(<10^{-4})	(0.041)	(0.105)	(0.130)	(0.003)	(0.0001)
	W	E	1.64	2.11	3.49	3.94	4.54	5.08	5.44	5.44
			(0.022)	(<10^{-4})	(<10^{-4})	(0.043)	(0.117)	(0.143)	(0.003)	(0.0002)
3b	V	D	1.86	2.94	3.13	3.69	4.65	4.66	4.85	5.07
			(<10^{-4})	(0.047)	(<10^{-4})	(<10^{-4})	(0.065)	(0.0008)	(<10^{-4})	(0.152)
	V	E	1.90	3.02	3.23	3.86	4.61	4.67	5.26	5.38
			(<10^{-4})	(0.050)	(<10^{-4})	(0.0001)	(0.0001)	(0.012)	(0.0004)	(0.515)
	W	D	2.12	2.64	3.44	3.50	4.42	4.95	5.24	5.44
			(<10^{-4})	(0.033)	(<10^{-4})	(<10^{-4})	(0.074)	(0.0002)	(0.383)	(0.002)
	W	E	2.15	2.73	3.54	3.66	4.60	5.16	5.40	5.54
			(<10^{-4})	(0.036)	(<10^{-4})	(<10^{-4})	(0.087)	(0.0003)	(0.409)	(0.002)
3c	V	D	1.43	2.69	3.03	3.48	4.11	5.05	5.37	5.45
			(0.007)	(0.0003)	(0.0002)	(0.016)	(0.105)	(0.303)	(0.0002)	(0.004)
	V	E	1.50	2.78	3.11	3.63	4.22	5.20	5.49	5.71
			(0.007)	(0.0003)	(0.0002)	(0.018)	(0.125)	(0.323)	(0.0002)	(0.005)
	W	D	1.42	2.84	3.14	3.47	4.10	5.07	5.34	5.49
			(0.006)	(0.0002)	(0.0004)	(0.016)	(0.117)	(0.279)	(0.0002)	(0.004)
	W	E	1.49	2.90	3.23	3.61	4.21	5.22	5.44	5.74
			(0.007)	(0.0001)	(0.0004)	(0.017)	(0.137)	(0.299)	(0.0002)	(0.005)
3d	V	D	1.70	2.87	3.09	3.80	4.12	5.12	5.30	5.52
			(0.017)	(0.0002)	(0.0001)	(0.069)	(0.123)	(0.276)	(0.0001)	(0.0002)
	V	E	1.77	2.95	3.20	3.90	4.27	5.26	5.39	5.77
			(0.019)	(0.0002)	(0.0002)	(0.092)	(0.124)	(0.291)	(0.0001)	(0.0001)
	W	D	1.69	2.99	3.27	3.79	4.14	5.13	5.25	5.55
			(0.018)	(0.0001)	(0.0003)	(0.078)	(0.121)	(0.269)	(0.0001)	(<10^{-4})
	W	E	1.76	3.05	3.38	3.89	4.29	5.27	5.33	5.80
			(0.019)	(0.0001)	(0.0003)	(0.100)	(0.123)	(0.282)	(0.0001)	(<10^{-4})

[a,b] See footnotes for Table 2.

of **3a**. According to the B3LYP/6-311+G(2d,p) results, **3d** was destabilized only by 0.6 kcal mol^{-1}. This would mean that about 25% of 5,6-indolequinone would exist in the gas phase as quinone methide. Adding diffuse function on hydrogen atoms in the 6-311++G(d,p) basis set resulted in a relative energy of 1.9 kcal mol^{-1} for **3d**. The PBE0 method with the same basis set yielded a similar value of 1.4 kcal mol^{-1} for the energy gap between **3a** and **3d**. However, even if we would take the largest energy difference of 1.9 kcal mol^{-1}, concentration of **3d** would be estimated around 4% which is still well above detection limits. The two other tautomers, **3b** and **3c**, were less favorable by 4−8 kcal mol^{-1} in comparison to **3a**. Both hybrid functionals used provided relative energies differing less than by 0.6 kcal mol^{-1}. Our SCRF calculation in water suggested significant destabilization of **3d** so that its energy became close to that of **3b**. Both tautomers were less favorable than **3a** by 7−9 kcal mol^{-1}. According to our best estimates obtained by calculating single-point energy at the geometry optimized in water, **3d** was destabilized by 8 kcal mol^{-1} relative to **3a** and its energy was practically identical to that of **3b**.

Our calculations suggest that **3c** is not present to an appreciable extent either in a vacuum or in water solution. It is interesting that this tautomer was frequently invoked into interpretation of experimental data. As mentioned above, intermediacy of **3c** in the oxidation of **2** was proposed in several pulse radiolysis studies.[4−7] No direct evidence for the formation of **3c** was obtained. Recently, the quinone imine formation was proposed as an explanation for the presence of two types of acidic functionalities in synthetic pigments obtained from **2**.[33] Variations in potentiometric titration curves and absorption spectra of the synthetic melanin pretreated Cu(II) and Zn(II) were interpreted as stabilization of this tautomer by coordination to the metal. It is very likely that metal binding affects the equilibrium between the tautomeric forms of the constituent monomers and it is also possible that oligomer formation influences this equilibrium. This will be examined in a future study. However, the protolytic equilibrium with pK_a ∼ 6 observed in ref 33 for synthetic melanins can be rationalized without invoking the formation of the quinone imine. This can be simply assigned to the nitrogen deprotonation in the quinone form **3a**. Notice that all four tautomers of **3** have the same common anion.

The fused ring system in **3a**−**3d** was completely planar. The quinonoid structures with alternating single and double C−C bonds, such as those shown in Figure 4, were predicted for all tautomers. A comparison of the bond lengths in indolequinones **3a**−**3d** and in dopachrome analogue **2f** suggested that contribution of zwitterionic resonance structures was relatively small even for the most polar tautomer **3a**. The two C−N bonds in **3a** were predicted to have similar length (1.382 Å and 1.392 Å for C_8−N and C_2−N), which was intermediate between that for the C_8−N bond in **2f** and the single C−N bonds in other molecules studied in this work (1.41−1.44 Å). The indolequinone compounds **3** are reactive and have not yet been isolated. The first observation of a relatively stable quinone characterized by UV absorption with a maximum around 360 nm was made almost fifty years ago by Beer et al.[34] in the reaction of 5,6-dihydroxy-2,3-dimethylindole with Ag_2O. NMR data confirming this assignment were reported by Prota and coworkers.[35] Recently, Sharma et al.[36] reported a crystal structure for mare lactoferrin that was presoaked in a solution of DOPA and tyrosinase. Two molecules designated in this paper as

indole-5,6-quinone were bound to the protein. In the pdb file (1F9B), the same molecules were referred to as 3H-indole-5,6-diol. Molecular geometry of these two species showed a striking deviation from planarity. The two C−O bonds (1.43−1.47 Å) appeared to be surprisingly long in comparison to the double bonds expected for the quinone (1.221 Å in **3a**). Thus, it remains unclear which species actually were bound and what might cause such a structural perturbation if they were isomers of **3** or **2**.

Excitation Energies of Tautomers of 5,6-Indolequinone (3). Table 4 presents the results of TD-DFT computations for 5,6-indolequinone tautomers. Vertical excitation energies were obtained with both the B3LYP and PBE0 method in the gas phase and water. When applied to **3**, the two techniques were in much better agreement than in the case of the tautomers of **2**. For the five lowest excited states, the excitation energies and oscillator strengths predicted with the PBE0 model were generally larger than those obtained with the B3LYP method, but the differences were relatively small (<0.15 eV for the energies and ≤10% for the intensities). The results of the two techniques for orientation of the transition dipole moments compared well for the first four excited states. An interesting finding of this study is the prediction of reasonably strong absorption in near-IR for the three of four tautomers of **3** (see Figure 5). The fourth tautomer, **3b**, showed only extremely weak absorption in the red region (∼2 eV) and a much stronger band corresponding to $S_0 \rightarrow S_2$ transition around 400−450 nm. The most intense bands in the electronic absorption spectra were predicted to be below 400 nm for all tautomers of **3**. The B3LYP and PBE0 results suggested that the most stable form **3a** may exhibit very strong solvatochromism because of the reversal of the energy order for the two lowest excited states. In the gas phase, the lowest excited state with energy of 1.82 eV (680 nm, here and below the PBE0 results are presented) corresponds to a very weak out-of-plane transition represented by a single excitation, HOMO → LUMO. The S_2 state with energy of 2.06 eV (603 nm) was characterized by much larger oscillator strength and a transition moment oriented almost parallel to the short pseudoaxis of the molecule. The orientation of the transition dipole moments for these two states was predicted to be essentially the same in a vacuum and in water, but the energy of the in-plane transition dropped down to 1.64 eV (758 nm) and that of the out-of-plane transition increased to 2.11 eV in aqueous solution. In contrast, no state reversal was predicted for the quinone methide **3d**. The lowest excited state of this molecule had practically identical energy (1.76−1.77 eV) and oscillator strength (0.019−0.018) in water and in the gas phase.

To assess performance of the selected DFT techniques in predicting electronic absorption spectra of quinones, we computed excitation energies of *o*-benzoquinone (**4**) at the same level of theory and compared them to available experimental data. The PBE0 method placed the lowest energy transition of **4** in $CHCl_3$ at 643 nm (1.93 eV, $f < 10^{-4}$). The two most intense transitions were predicted at 413 nm (3.00 eV, $f = 0.04$) and 228 nm (5.43 eV, $f = 0.05$). The B3LYP excitation energies were slightly smaller for all states considered. The PBE0 results were in reasonable agreement with a measured spectrum of **4** in $CHCl_3$ which showed three maxima at 590 nm (2.10 eV, log ϵ =1.48), 375 nm (3.31 eV, log $\epsilon = 3.23$), and 260 nm (4.77 eV, log $\epsilon = 3.11$).[37] Clearly, a quantitative comparison of the energies corresponding to the maxima in the absorption spectra measured in solution with computational data for the vertical excitation energies is rather problematic. Nevertheless, our results for **4** seemed to be rather encouraging and indicative of possibility to utilize TD-DFT data for semiquantitative analysis of spectroscopic properties of **3**.

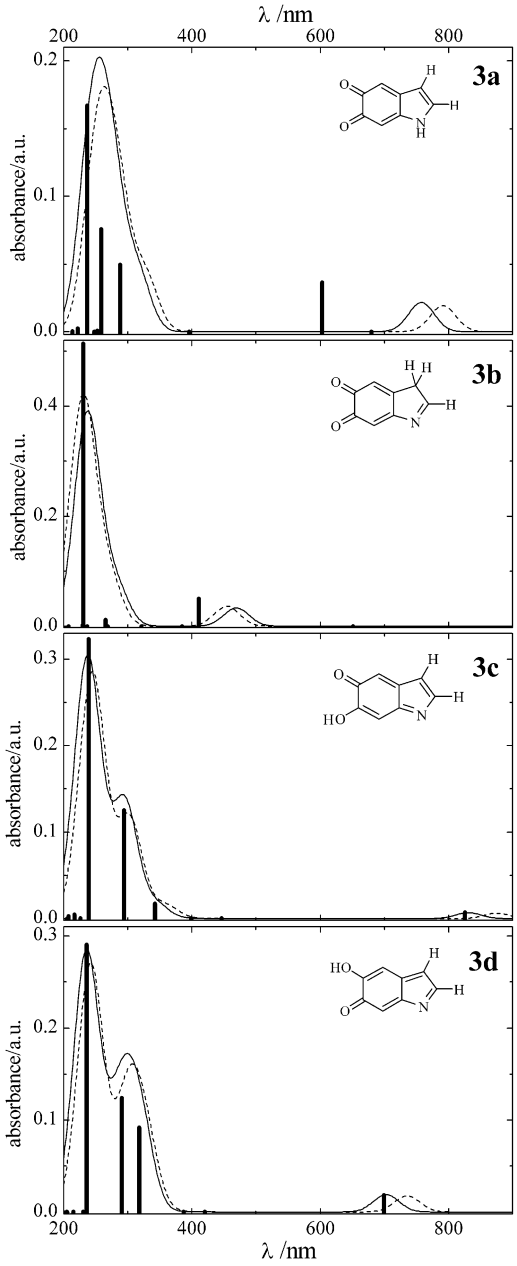

Figure 5. Calculated absorption spectra of tautomers of **3** in the gas phase (vertical bars) and in aqueous solution (solid and dashed lines). The spectra in solution were simulated by using Gaussian envelopes centered at the computed absorption maxima with arbitrary width of 20 nm and amplitude equal to the oscillator strength. The PBE0 (solid) and B3LYP method (dashed) were used in combination with the 6-311+G(d,p) basis set and the CPCM model.

As mentioned above, a relative stable product of 5,6-dihydroxy-2,3-dimethylindole oxidation could be identified as the corresponding indolequinone. This compound was characterized by absorption peaked at ∼360 nm.[34,35] These findings are in contrast to the results of pulse radiolysis studies[4−7] which suggested that a primary product of the bimolecular reaction of semiquinone radicals responsible for the absorption around 430 nm was a corresponding indolequinone or its tautomers. Our TD-DFT computations predicted for 5,6-indolequinone in water to exist almost exclusively as a single tautomer **3a** with no significant absorption in the range 400−600 nm but with relatively strong transitions at 327 nm (3.80 eV) and 282 nm (4.40 eV). Quinone methide **3d** was strongly destabilized in

polar solvents and therefore should not contribute to the measured absorption spectrum. Even if one would assume that concentration of **3d** was significant in water, it could not be responsible for 430 nm absorption observed (see Figure 5). The only tautomer that was found to absorb around 430 nm was **3b**, but it was strongly disfavored both in the gas and in water. The calculated difference between energies of **3a** and **3b** (6−9 kcal mol^{-1}) is definitely larger than the expected accuracy of the techniques used. By comparing simulated spectra of the tautomers of **2** and **3** with those reported in pulse radiolysis studies, one could suggest that the chromophore of **2e** might be responsible for 430 nm absorption. This would mean that the major reaction of two semiquinone radicals was not disproportionation as it has been suggested but dimerization leading mainly to 2,2′-diindole in the tautomeric form corresponding to **2e**. Subsequent tautomerization of the dimer could account for an H/D isotope effect observed.[7] It is noteworthy that 2,2′- and 2,4′−diindole were identified as the major components of complex mixtures obtained by oxidation of **2** under various conditions.[1] It would be of interest to repeat transient absorption studies of oxidation of **2** and to record spectra in the red and near-IR range. Considering a significant difference in solvent effects predicted for **3a** and **3d**, these data should allow unambiguous identification of the transients and clarification of the oxidation mechanisms.

Conclusions

The computational results obtained at different levels of theory provided a qualitatively consistent picture of tautomerization equilibria for **2** and **3**. Our data showed that **2a** corresponding to the generally accepted structure is the most stable tautomer in both gas phase and aqueous solution. Quinone methide **2e** was the most favorable among the minor tautomers of **2**. Our best estimate for its energy in water relative to that of **2a** was 6 kcal mol^{-1}. In contrast, our DFT data for indolequinone **3** suggested that this compound in the gas phase should exist as a mixture of two tautomers **3a** (quinone) and **3d** (quinone methide). Relative concentration of **3d** was predicted to be definitely within detection limits. However, the energy gap between **3a** and **3d** increased substantially in solution so that the concentration of **3d** should be negligible in polar solvents.

Vertical excitation energies for tautomers of **2** and **3** in solutions were obtained by combining TD-DFT techniques with the SCRF calculation. Simulated absorption spectra in water were in semiquantitative agreement with available experimental data. Relatively strong absorption in near-IR range was predicted for **3**. It is suggested that this spectral feature might be used to clarify the complex mechanisms of dihydroxyindole oxidation.

Acknowledgment. We acknowledge the support of North Carolina Supercomputing Center, Kansas NSF Cooperative Agreement EPS-9874732, the Wichita State University High Performance Computing Center, the National Institute of General Medical Sciences, and Unilever Research US.

Supporting Information Available: Cartesian coordinates for molecules **2a**−**2i**, **3a**−**3d**, **4** (ASCII), Table 1S, and Table 2S with the total energies. This material is available free of charge via the Internet at http://pubs.acs.org.

References and Notes

(1) Prota, G. *Melanins and Melanogenesis*; Academic Press: San Diego, CA, 1992; 290 p.

(2) Ito, S. In *The Pigmentary System: Physiology and Pathophysiology*; Norlund, J. J., Boissy, R. E., Hearing, V. J., King, R. A., Ortonne, J. P., Eds.; Oxford University Press: New York, 1998; pp 439−450.

(3) Wakamatsu, K.; Ito, S. *Pigm. Cell Res.* **2002**, *15*, 174−183.

(4) Lambert, C.; Chacon, J. N.; Chedekel, M. R.; Land, E. J.; Riley, P. A.; Thompson, A.; Truscott, T. G. *Biochim. Biophys. Acta* **1989**, *993*, 12−20.

(5) (a) Al-Kazwini, A. T.; O'Neill, P.; Adams, G. E.; Cundall, R. B.; Jacquet, B.; Lang, G.; Junino, A. *J. Phys. Chem.* **1990**, *94*, 6666−6670. (b) Al-Kazwini, A. T.; O'Neill, P.; Adams, G. E.; Cundall, R. B.; Lang, G.; Junino, A. *J. Chem. Soc., Perkin Trans. 2* **1991**, *12*, 1941−1945.

(6) (a) Al-Kazwini, A. T.; O'Neill, P.; Cundall, R. B.; Adams, G. E.; Junino, A.; Maignan, J.. *Tetrahedron Lett.* **1992**, *33*, 3045−3048. (b) Al-Kazwini, A. T.; O'Neill, P.; Adams, G. E.; Cundall, R. B.; Junino, A.; Maignan, J. *J. Chem. Soc,. Perkin Trans. 2*, **1992**, 657−661.

(7) Lambert. C.; Land. E. J.; Riley. P. A.; Truscott, T. G. *Biochim. Biophys. Acta* **1990**, *1035*, 319−324.

(8) (a) Pullman, A.; Pullman, B. *Biochim. Biophys. Acta* **1961**, *54*, 384−385. (b) Pullman, B. *Biochim. Biophys. Acta* **1963**, *66*, 164−165.

(9) (a) Galvão, D. S.; Caldas, M. J. *J. Chem. Phys.* **1988**, *88*, 4088−4091. (b) Galvão, D. S.; Caldas, M. J. *J. Chem. Phys.* **1990**, *92*, 2630−2636. (c) Galvão, D. S.; Caldas, M. J. *J. Chem. Phys.* **1990**, *93*, 2848−2853.

(10) Bolívar-Marinez, L. E.; Galvão, D. S.; Caldas, M. J. *J. Phys. Chem. B* **1999**, *103*, 2993−3000.

(11) Stark, K. B.; Gallas, J. M.; Zajac, G. W.; Eisner, M.; Golab, J. T. *J. Phys. Chem. B* **2003**, *107*, 3061−3067.

(12) Frisch, M. J.; Trucks, G. W.; Schlegel, H. B.; Scuseria, G. E.; Robb, M. A.; Cheeseman, J. R.; Zakrzewski, V. G.; Montgomery, J. A., Jr.; Stratmann, R. E.; Burant, J. C.; Dapprich, S.; Millam, J. M.; Daniels, A. D.; Kudin, K. N.; Strain, M. C.; Farkas, O.; Tomasi, J.; Barone, V.; Cossi, M.; Cammi, R.; Mennucci, B.; Pomelli, C.; Adamo, C.; Clifford, S.; Ochterski, J.; Petersson, G. A.; Ayala, P. Y.; Cui, Q.; Morokuma, K.; Malick, D. K.; Rabuck, A. D.; Raghavachari, K.; Foresman, J. B.; Cioslowski, J.; Ortiz, J. V.; Stefanov, B. B.; Liu, G.; Liashenko, A.; Piskorz, P.; Komaromi, I.; Gomperts, R.; Martin, R. L.; Fox, D. J.; Keith, T.; Al-Laham, M. A.; Peng, C. Y.; Nanayakkara, A.; Gonzalez, C.; Challacombe, M.; Gill, P. M. W.; Johnson, B. G.; Chen, W.; Wong, M. W.; Andres, J. L.; Head-Gordon, M.; Replogle, E. S.; Pople, J. A. *Gaussian 98*, revision A.11; Gaussian, Inc.: Pittsburgh, PA, 1998.

(13) Becke, A. D. *J. Chem. Phys.* **1993**, *98*, 5648−5652.

(14) (a) Lee, C.; Yang, W.; Parr, R. G. *Phys. Rev. B* **1988**, *37*, 785−797. (b) Stephens, P. J.; Devlin, F. J.; Chabalowski, C. F.; Frisch, M. J. *J. Phys. Chem.* **1994**, *98*, 11623−11627.

(15) (a) Perdew, J. P.; Burke, K.; Ernzerhof, M. *Phys. Rev. Lett.* **1996**, *77*, 3865−3868. (b) Perdew, J. P.; Burke, K.; Ernzerhof, M. *Phys. Rev. Lett.* **1997**, *78*, 1396−1396.

(16) (a) Adamo, C.; Barone, V. *Chem. Phys. Lett.* **1998**, *298*, 113−119. (b) Adamo, C.; Barone, V. *J. Chem. Phys.* **1999**, *110*, 6158−6170. (c) Ernzerhof, M.; Scuseria, G. E. *J. Chem. Phys.* **1999**, *110*, 5029−5036.

(17) Casida, M. E.; Jamorski, C.; Casida, K. C.; Salahub, D. R. *J. Chem. Phys.* **1998**, *108*, 4439−4449.

(18) Barone, V.; Cossi, M. *J. Phys. Chem.* **1998**, *102*, 1995−2001.

(19) (a) Gill, P. M. W.; Johnson, B. G.; Pople, J. A.; Frish, M. J. *Chem. Phys. Lett.* **1992**, *197*, 499−505. (b) Johnson, B. G.; Gill, P. M. W.; Pople, J. A. *J. Chem. Phys.* **1993**, *98*, 5612−5626. (c) Curtiss, L. A.; Raghavachari, K.; Redfern, P. C.; Pople, J. A. *J. Chem. Phys.* **1997**, *106*, 1063−1079.

(20) Kohn, W.; Becke, A. D.; Parr, R. G. *J. Phys. Chem.* **1996**, *100*, 12974−12980 and references therein.

(21) (a) Rice B. M.; Chabalowski C. F. *J. Phys. Chem. A* **1997**, *101*, 8720−8726. (b) Wu, C. J.; Fried, L. E. *J. Phys. Chem. A* **1997,** *101*, 8675−8679. (c) Harris, N. J.; Lammertsma, K. *J. Am. Chem. Soc.* **1997**, *119*, 6583−6589. (d) Mohandas, P.; Umapathy, S. *J. Phys. Chem. A* **1997**, *101*, 4449−4459. (e) Alcami, M.; Mo, O.; Yanez, M.; Cooper, I. L. *J. Chem. Phys.* **2000**, *112*, 6131−6140. (f) Bernardi, F.; Bottoni, A.; Garavelli, M. *Quant. Struct.−Act. Relat.* **2002**, *21*, 128−148.

(22) Il'ichev, Yu. V.; Wirz, J. *J. Phys. Chem. A* **2000**, *104*, 7856−7870 and references therein.

(23) Scott, A. P.; Radom, L. *J. Phys. Chem.* **1996**, *100*, 16502−16513.

(24) Takigawa, T.; Ashida, T.; Sasado, Y.; Kakuda, M. *Bull. Chem. Soc. Jpn.* **1966**, *39*, 2369−2378.

(25) (a) Slater, L. S.; Callis, P. R. *J. Phys. Chem.* **1995**, *99*, 8572−8581. (b) Serrano-Andres, L.; Roos, B. *J. Am. Chem. Soc.* **1996**, *118*, 185−195.

(26) Il'ichev, Yu. V., unpublished data.

(27) (a) Cheng, A. C.; Shulgin, A. T.; Castagnoli, N., Jr. *J. Org. Chem.* **1982**, *47*, 5258−5262. (b) Sugumaran, M.; Dali, H.; Semensi, V. *Bioorg. Chem.* **1990**, *18*, 144−153. (c) Crescenzi, O.; Costantini, C.; Prota, G. *Tetrahedron Lett.* **1990**, *31*, 6095−6096.

(28) Costantini, C.; Crescenzi, O.; Prota, G. *Tetrahedron Lett.* **1991**, *32*, 3849−3850.

(29) (a) Adamo, C.; Scuseria, G. E.; Barone, V. *J. Chem. Phys.* **1999**, *111*, 2889−2899. (b) Adamo, C.; Barone, V. *Chem. Phys. Lett.* **2000**, *330*, 152−160. (c) Guillemoles, J.-F.; Barone, V.; Joubert, L.; Adamo, C. *J. Phys. Chem. A* **2002**, *106*, 11354−11360.

(30) Mason, H. S.; Peterson, E. W. *Biochim. Biophys. Acta* **1965**, *111*, 134−146.

(31) (a) Albinsson, B.; Kubista, M.; Norden, B.; Thulstrup, E. W. *J. Phys. Chem.* **1989**, *93*, 6646−6654. (b) Albinsson, B.; Norden, B. *J. Phys. Chem.* **1992**, *96*, 6204−6212.

(32) Al-Kazwini, A. T.; O'Neill, P.; Adams, G. E.; Cundall, R. B.; Maignan, J.; Junino, A. *J. Chem. Soc., Perkin Trans. 2* **1996**, 241−245.

(33) (a) Szpoganicz, B.; Gidanian, S.; Kong, P.; Farmer, P. *J. Inorg. Biochem.* **2002**, *89*, 45−53. (b) S. Gidanian, P. J. Farmer, *J. Inorg. Biochem.* **2002**, *89*, 54−60.

(34) Beer, R. J. S.; Broadhurst, T.; Robertson, A. *J. Chem. Soc.* **1954**, 1947−1954.

(35) Napolitano, A.; Pezzella, A.; d'Ischia, M.; Prota, G. *Tetrahedron Lett.* **1996**, *37*, 4241−4242.

(36) Sharma, A. K.; Kumar, S.; Sharma, V.; Nagpal, A.; Singh, N.; Tamboli, I.; Mani, I.; Raman, G.; Singh, T. P. *Proteins* **2001**, *45*, 229−236.

(37) Engelhard, M.; Luettke, W. *Chem. Ber.* **1977**, *110*, 3759−3769.